

# Detection of supraventricular and ventricular ectopic beats using a single lead ECG

Philip de Chazal, *Member, IEEE*

**Abstract**— Two simple algorithms for supraventricular (SVEB) and ventricular ectopic beat (VEB) detection using the electrocardiogram (ECG) are presented. Both algorithms use time-domain features and a linear classifier. The first algorithm requires QRS detection only and the second algorithm requires P, QRS and T wave segmentation. Data was obtained from the 44 non-pacemaker recordings of the MIT-BIH arrhythmia database and contained approximately 100,000 beats. Performance assessment of the best system resulted in an accuracy of 94.4% when discriminating SVEB from non-SVEBs and 97.8% in discriminating VEB from non-VEBs.

## I. INTRODUCTION

Detection of nonlife threatening arrhythmias is an important area of study as many of these arrhythmias may require therapy to prevent further problems. Sensing of these arrhythmias can be achieved using the low cost, non-invasive electrocardiogram (ECG). It is an effective test for arrhythmia analysis and has become the standard diagnostic tool. Some arrhythmias appear infrequently and up to a month of ECG activity may need to be recorded using a Holter ECG monitor to successfully capture them. Many arrhythmias manifest as sequences of heart-beats with unusual timing or ECG morphology. An important step towards identifying an arrhythmia is the classification of heart-beats. The rhythm of the ECG signal can then be determined by knowing the classification of consecutive heart-beats in the signal [1]. Manual annotation of beat-types of multiday of ECG recordings is time consuming so any automated processing of the ECG that labels beat-types is of assistance to clinician and is the focus of this study.

Research into this heartbeat classification has been an active area for many years and resulted in numerous publications e.g. [4]-[15]. A variety of approaches have been considered by other researchers. Discriminating features for separating the heartbeat classes have included Hermite functions [2],[5],[9], statistical features [5],[13], waveform morphology [4],[6],[8],[11]-[15] and wavelets [7],[10],[15]. Classification methods include artificial neural networks [9],[10], decision trees [6], linear discriminants [4],[8],[11],[14], self organizing feature maps [2], support vector machines [5],[7],[15] and other statistically motivated approaches [12],[13].

Approaches using wavelets, statistical features, artificial neural networks and support vector machines are expensive

from a computational viewpoint. The purpose of this study was to investigate low computational cost algorithms using a single ECG lead that maybe suitable for real-time implementation on power limited devices such as Holter ECG recorders.

## II. METHODS

### A. Data

Data from the MIT-BIH arrhythmia database [16] was used in this study. The database contains 48 recordings each containing two ECG lead signals (denoted lead A and B). For this study we focused on using lead A only. In 45 recordings lead A is modified lead II and for the other three is lead V5. Following AAMI recommended practice [17],[18] the four paced beat recordings were removed from the analysis.

The data is band-pass filtered at 0.1-100Hz and sampled at 360Hz. There are over 109,000 labeled ventricular beats from 15 different heart-beat types which were remapped to the five AAMI heart-beat classes [17], [18] using the mapping in [4]. Class N contained beats originating in the sinus node (normal and bundle branch block beat types), class S contained supraventricular ectopic beats (SVEB), class V contained ventricular ectopic beats (VEB), class F contained beats that result from fusing normal and VEBs, and class Q contained unknown beats including paced beats.

### B. Data Processing

Fig. 1 shows an automated system suitable for heartbeat classification arising from this project. There are three stages: a pre-processing stage, a processing stage, and a classification stage. The system processes a single lead ECG signal and assigns each heartbeat to one of the five AAMI beat classes.

The pre-processing stage receives a digital ECG signal and removes artifact signals from the ECG signal by applying a filtering unit. Artifact signals include high frequency noise, power line interference and baseline wander. Filters for these stages are described in [4]. The processing stage consists of heartbeat detection and feature extraction phases. The heartbeat detection module aims to locate all heartbeats. In this study the manually verified heartbeat fiducial point times provided with the MIT-BIH arrhythmia database were utilised. Heartbeat segmentation follows heartbeat detection to provide the QRS onset and offset and T-wave offset times; a Boolean value indicating the presence/absence of a P-wave and, if present, the P-wave onset and offset time for each heartbeat fiducial point.

\*Research supported by Australian Research Council grant number FT110101098.

P. de Chazal is with the Marcs Institute, University of Western Sydney, Australia (Phone: +61 2 4736 0447; fax: +61 2 4736 0833; e-mail: p.dechazal@uws.edu.au).

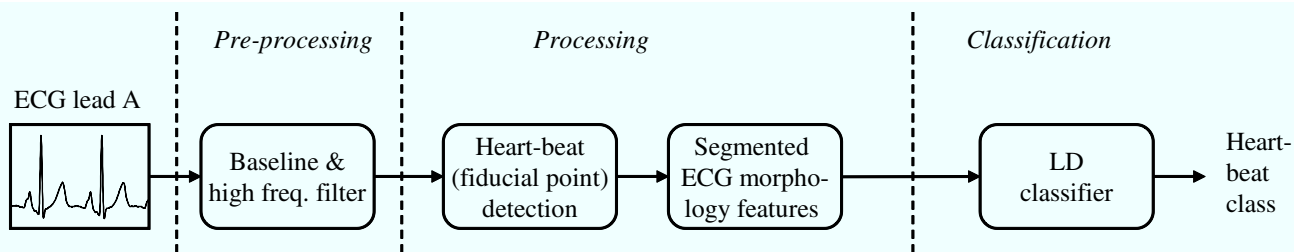


Figure 1: Schematic representation of the automated processing of the single lead ECG for classification of heart-beats.

TABLE I. THE A) FEATURES GROUPS AND B) FEATURE SETS CONSIDERED IN THIS STUDY.

Group Label	Features	Group Label	Features
A)	RR intervals <ul style="list-style-type: none"> <li>• Pre-RR interval</li> <li>• Post-RR interval</li> <li>• Average RR-interval</li> <li>• Local avg. RR-interval</li> </ul>	Segmented Morphology	<ul style="list-style-type: none"> <li>• ECG morphology (10 samples) between QRS onset and QRS offset</li> <li>• ECG morphology (9 samples) between QRS offset and T-wave offset</li> </ul>
	Heart-beat intervals <ul style="list-style-type: none"> <li>• QRS duration (QRS offset -QRS onset)</li> <li>• T-wave duration (T-wave offset - QRS offset)</li> <li>• P wave flag</li> </ul>	Fixed Interval Morphology	<ul style="list-style-type: none"> <li>• ECG morphology (10 samples) between FP-50ms to FP+100ms</li> <li>• ECG morphology (9 samples) between between FP-150ms to FP+500ms</li> </ul>
<hr/>			
		Number of Features	
B)	Feature Set	Feature Groups	
	FS1	RR intervals, Heart-beat intervals, Segmented Morphology	26
	FS2	RR intervals, Fixed Interval Morphology	22

For each heartbeat the feature extraction phase forms a feature vector that is processed by the classifier stage. In response to the input feature vector, the classification stage selects one of the required classes. The classifier contains parameters that are set during the system development to optimise the classification performance. The feature extraction phase and the classification stage are discussed in more detail below.

### B. Feature extraction

The ECG heart-beat segmentation program of Laguna et al<sup>1</sup> was used to provide estimates of heart-beat segmentation points i.e. the QRS onset and offset and T-wave offset times; a Boolean value indicating the presence/absence of a P-wave and, if present, the P-wave onset and offset time for each heart-beat fiducial point. The program has been validated on the CSE multilead database [19] and the MIT-BIH QT database [20] and the accuracy of the system in determining

heart-beat segmentation points was comparable with the inter-expert variation.

Feature extraction is based on the methods employed in [4]. Features relating to fiducial point intervals, heart beat intervals and ECG morphology were calculated for each heartbeat. Table I lists the features used in this study.

#### 1) RR-interval features

Heartbeat fiducial point intervals (henceforth called RR-intervals) were defined as the interval between successive heartbeat fiducial points (the time interval between successive major local extrema). Four features (Table IA: RR-intervals) were extracted from the RR sequence. The pre-RR-interval was the RR-interval between a given heartbeat and the previous heartbeat. The post-RR-interval was the RR-interval between a given heartbeat and the following heartbeat. The average RR-interval was the mean of the valid RR-intervals for a recording and had the same value for all heartbeats in a recording. Finally, the local average RR-interval was determined by averaging the valid RR-intervals of the ten RR-intervals surrounding a heartbeat.

<sup>1</sup>“ecgpuwave”: see <http://www.physionet.org/physiotools/software-index.shtml>

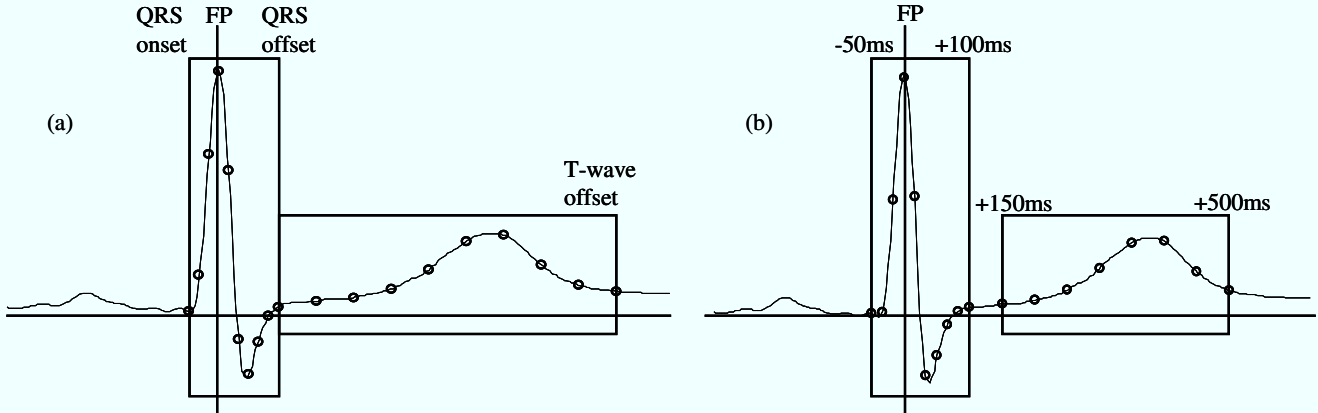


Fig. 2: Two time-sampling methods for extracting ECG morphology features. (a) Segment Morphology: after determining the fiducial point (FP), the QRS onset and offset and T-wave offset points are found. Ten evenly spaced samples of the ECG between the QRS onset and offset and nine evenly spaced samples of the ECG between the QRS offset and T-wave offset are extracted. These features were used in FS1. (b) Fixed Interval Morphology: after determining the FP, nine samples of the ECG between FP-50ms and FP+100ms and nine samples between FP+150ms and FP+500ms are extracted. These features were used in FS2.

### 1) Heartbeat interval features

Three features per ECG lead (Table IA: Heartbeat interval) relating to heartbeat intervals were calculated after heartbeat segmentation. The QRS duration was the time interval between the QRS onset and the QRS offset. The T-wave duration was defined as the time interval between the QRS offset and the T-wave offset. The third feature was a Boolean variable indicating the presence or absence of a P-wave.

### 2) Segmented morphology features

The segmented morphology group (Table IA: Segment Morphology) contained amplitude values of the ECG signal determined by a sampling window between the QRS onset and offset and a sampling window between the QRS offset and the T-wave offset points. Ten features were derived by uniformly sampling the ECG amplitude in the first window and nine features were derived by uniformly sampling the second window (Figure 2a).

### 3) Fixed interval morphology features

The segmented morphology group (Table IA: Segment Morphology) contained amplitude values of the ECG signal determined by a sampling window between the QRS onset and offset and a sampling window between the QRS offset and the T-wave offset points. Ten features were derived by uniformly sampling the ECG amplitude in the first window and nine features were derived by uniformly sampling the second window (Figure 2b).

### C. Feature sets

Two feature set were considered (see Table 1B). The first feature set (FS1) required P, QRS and T wave segmentation followed by wave morphology sampling. While the second (FS2) required QRS detection followed by wave morphology sampling. FS2 required significantly less computation than FS1.

### D. Classifier

Classifier models based on linear discriminants (LD) were utilised throughout this study. The model parameters  $\mu_k$  - class conditional mean vectors and  $\Sigma$  - common covariance matrix were determined using the training data using 'plug-in' maximum likelihood estimates [21].

### E. Performance Estimation

The same data division scheme as used in [4] was used. Classifier training was achieved using data from 22 recordings of the database (DS1 in [4]) and performance assessment was determined using the other 22 recordings (DS2 in [4]). Performance measures considered were the accuracy, sensitivity, positive predictivity and false positive ratio for VEB and SVEB beat classes. The 5-way beat-by-beat performance is also presented. Definitions for these measures may be found in [4].

## III. RESULTS AND DISCUSSION

The SVEB and VEB classification performance figures are shown in Table II for the two classifier configurations considered in this study. The beat-by-beat performance for FS2 is shown in Table III.

FS2 outperformed FS1 for both SVEB and VEB detection suggesting that P wave, QRS onset and offset and T wave offset information did not aid the beat classification problem.

For FS2, the overall accuracy for SVEB detection was 94.4% with a sensitivity of 73.5%, a positive predictivity of 37.0% and a false positive ratio of 4.8%. Comparison with other published detectors reveals that the detector has similar SVEB performance (e.g. [4] Acc: 94.6%, Se: 75.9%, +P 38.5%; [11] Se: 77%, +P: 39%; [15] Se: 60.8%, +P 52.3%).

The overall accuracy for VEB detection was 97.8% with a sensitivity of 87.6%, a positive predictivity of 80.3% and a

TABLE II. A) SVEB AND VEB PERFORMANCE MEASURES FOR FEATURE SETS FS1 AND FS2. B) BEAT-BY-BEAT CLASSIFICATION TABLE FOR FS2.

	SVEB				VEB			
	Acc(%)	Se(%)	+P(%)	FPR(%)	Acc(%)	Se(%)	+P(%)	FPR(%)
A) FS1	93.6	61.2	31.2	5.2	95.4	72.4	62.3	3.0
FS2	94.4	73.5	37.0	4.8	97.8	87.6	80.3	1.5

B)	Reference	Algorithm				
		n	s	v	f	q
	N	40455	2089	298	1328	88
	S	82	1352	393	10	0
	V	49	209	2820	129	14
	F	228	4	11	72	73
	Q	4	0	1	0	2

false positive ratio of 1.5%. Comparison with other published detectors shows the VEB performance is comparable to others (e.g. [4] Acc: 97.4%, Se: 77.7%, +P 81.9%; [11] Se: 81%, +P 87%; [15] Se: 81.5%, +P 63.1%). Thus there is no performance loss when using a low cost computational algorithm.

Benefits of the proposed algorithm are that its low computational cost may allow real-time implementation on a power limited devices such as Holter ECG recorders and therefore reduce the time period of arrhythmia detection without loss in detection accuracy.

#### IV. CONCLUSION

The objective of this study was to develop a supraventricular and ventricular ectopic heartbeat detection using a single lead ECG with low computational cost and suitable for real-time implementation. The study focused on two sets of time-domain features. The simplest system required QRS detection for each heartbeat followed by wave morphology sampling. The second system required P wave detection, QRS detection, QRS onset and offset detection and T wave offset detection. It also required wave morphology sampling. The first system outperformed the second system and was comparable to other published systems. These result shows that a supraventricular and ventricular ectopic heartbeat detection can be designed with low computational requirements.

#### REFERENCES

- [1] J.A. Kastor, *Arrhythmias*. 2nd Edition, London: W. B. Saunders, 1994.
- [2] M. Lagerholm, C. Peterson, G. Braccini, L. Edenbrandt, and L. Sornmo, "Clustering ECG complexes using Hermite functions and self-organizing maps," *IEEE Trans. Biomed. Eng.*, vol. 47, no. 7, pp. 838–848, Jul. 2000.
- [3] G. K. Prasad and J. S. Sahambi, "Classification of ECG arrhythmias using multi-resolution analysis and neural networks," in *Proc. Conf. Convergent Technol. Asia-Pacific Region*, Oct. 2003, pp. 227–231.
- [4] P. de Chazal, M. O. Dwyer, and R. B. Reilly, "Automatic classification of heartbeats using ECG morphology and heartbeat

- interval features," *IEEE Trans. Biomed. Eng.*, vol. 51, no. 7, pp. 1196–1206, Jul. 2004.
- [5] S. Osowski, L. T. Hoa, and T. Markiewicz, "Support vector machine-based expert system for reliable heartbeat recognition," *IEEE Trans. Biomed. Eng.*, vol. 51, no. 4, pp. 582–589, Apr. 2004.
- [6] J. Rodriguez, A. Goni, and A. Illarramendi, "Real-time classification of ECGs on a PDA," *IEEE Trans. Info. Tech. Biomed.*, vol. 9, no. 1, pp. 23–34, Mar. 2005.
- [7] X. Jiang, L. Q. Zhang, Q. B. Zhao, and S. Albayrak, "ECG arrhythmias recognition system based on independent component analysis feature extraction," in *Proc. IEEE Region 10 Conf.*, Nov. 2006, pp. 1–4.
- [8] P. de Chazal and R. B. Reilly, "A patient-adapting heartbeat classifier using ECG morphology and heartbeat interval features," *IEEE Trans. Biomed. Eng.*, vol. 53, no. 12, pp. 2535–2543, Dec. 2006.
- [9] W. Jiang and G. S. Kong, "Block-based neural networks for personalized ECG signal classification," *IEEE Trans. Neural Networks*, vol. 18, no. 6, pp. 1750–1761, Nov. 2007.
- [10] T. Ince, S. Kiranyaz, and M. Gabbouj, "A generic and robust system for automated patient-specific classification of ECG signals," *IEEE Trans. Biomed. Eng.*, vol. 56, no. 5, pp. 1415–1426, May 2009.
- [11] M. Llamedo and J. P. Martinez, "Heartbeat classification using feature selection driven by database generalization criteria," *IEEE Trans. Biomed. Eng.*, vol. 58, no. 3, pp. 616–625, Mar. 2011.
- [12] L. de Oliveira, R. Andreao, and M. Sarcinelli, "Premature Ventricular beat classification using a dynamic Bayesian network," in *Proc. IEEE Int. Conf. Eng. Med. Biol. Soc., Aug./Sep. 2011*, pp. 4984–4987.
- [13] G. de Lannoy, D. Francois, J. Delbeke, and M. Verleysen, "Weighted conditional random fields for supervised interpatient heartbeat classification," *IEEE Trans. Biomed. Eng.*, vol. 59, no. 1, pp. 241–247, Jan. 2012.
- [14] A.S. Alvarado, C. Lakshminarayan and J.C. Principe, "Time-based compression and classification of heartbeats," *IEEE Trans. Biomed. Eng.*, vol. 59, no. 6, pp. 1641–1648, June. 2012.
- [15] C. Ye, B.V.K. Vijaya Kumar, M.T. Coimbra, "Heartbeat classification using morphological and dynamic features of ECG signals," *IEEE Trans. Biomed. Eng.*, vol. 59, no. 10, pp. 2930–2941, Oct. 2012.
- [16] R. Mark and G. Moody, *MIT-BIH Arrhythmia Database*, 3rd Edition." May, 1997.
- [17] ANSI-AAMI EC57:1998 (American National Standard). *Testing and reporting performance results of cardiac rhythm and ST segment measurement algorithms*. Association for the Advancement of Medical Instrumentation, Arlington, VA, 1998.
- [18] ANSI ECAR:1987. *Recommended practice for testing and reporting performance results of ventricular arrhythmia detection algorithms*, Association for the Advancement of Medical Instrumentation, Arlington, VA, 1987.
- [19] P. Laguna, R. Jané, P. Caminal, "Automatic Detection of Wave Boundaries in Multilead ECG Signals: Validation with the CSE Database," *Computers and Biomedical Research*, vol 27(1):45-60, 1994.
- [20] R Jané R, A. Blasi, J. García, P. Laguna, "Evaluation of an automatic threshold based detector of waveform limits in Holter ECG with the QT database," in *Computers in Cardiology*, vol. 24, pp. 295-298, 1997.
- [21] B.D. Ripley, *Pattern Recognition and Neural Networks*, Cambridge, England: Cambridge University Press, 1996.